HHS Public Access

Author manuscript

J Nat Prod. Author manuscript; available in PMC 2023 September 05.

Published in final edited form as:

J Nat Prod. 2022 March 25; 85(3): 657–665. doi:10.1021/acs.jnatprod.2c00015.

Marine natural products as leads against SARS-CoV-2 infection

Bhuwan Khatri Chhetri[†,a], **Philip R. Tedbury**[▽,a], **Anne Marie Sweeney-Jones**[†], **Luke Mani**[ξ], **Katy Soapi**[ξ], **Candela Manfredi**[¶], **Eric Sorscher**[¶], **Stefan G. Sarafianos**[▽], **Julia Kubanek**[*,†,‡,§,Θ]

[†]School of Chemistry and Biochemistry, Georgia Institute of Technology, Atlanta, GA 30332, USA

[‡]Center for Microbial Dynamics and Infection, Georgia Institute of Technology, Atlanta, GA 30332, USA

[§]School of Biological Sciences, Georgia Institute of Technology, Atlanta, GA 30332, USA

[▽]Laboratory of Biochemical Pharmacology, Department of Pediatrics, Emory University School of Medicine, Atlanta, GA 30322, USA

[ξ]Institute of Applied Sciences, University of South Pacific, Suva, Fiji

[¶]Department of Pediatrics, Division of Pulmonary Medicine, Emory University School of Medicine, Atlanta, GA 30322, USA.

[Θ]Parker H. Petit Institute for Bioengineering and Bioscience, Georgia Institute of Technology, Atlanta, GA 30332, USA

Abstract

Since early 2020, disease caused by the severe acute respiratory syndrome coronavirus 2 (SARS-CoV-2) has become a global pandemic causing millions of infections and deaths worldwide. Despite rapid deployment of effective vaccines, it is apparent that the global community lacks multipronged interventions to combat viral infection and disease. A major limitation is the paucity of antiviral drug options representing diverse molecular scaffolds and mechanisms of action. Here we report the antiviral activities of three distinct marine natural products: homofascaplysin A (**1**), (+)-aureol (**2**), and bromophycolide A (**3**), evidenced by their ability to inhibit SARS-CoV-2 replication at concentrations that are non-toxic towards human airway epithelial cells. These compounds stand as promising candidates for further exploration towards the discovery of novel drug leads against SARS-CoV-2.

Graphical Abstract

[*]Corresponding author julia.kubanek@biosci.gatech.edu.
[a]These authors contributed equally

Supporting information

The Supporting Information is available free of charge on the ACS Publications website at DOI:
Structure of natural products with promising antiviral activity including SARS-CoV, picture of *F. reticulata,* compound characterization data, ^{1}H NMR and HRMS spectra of bioactive/isolated compounds, X-ray crystallographic data.

The authors declare no competing financial interest.

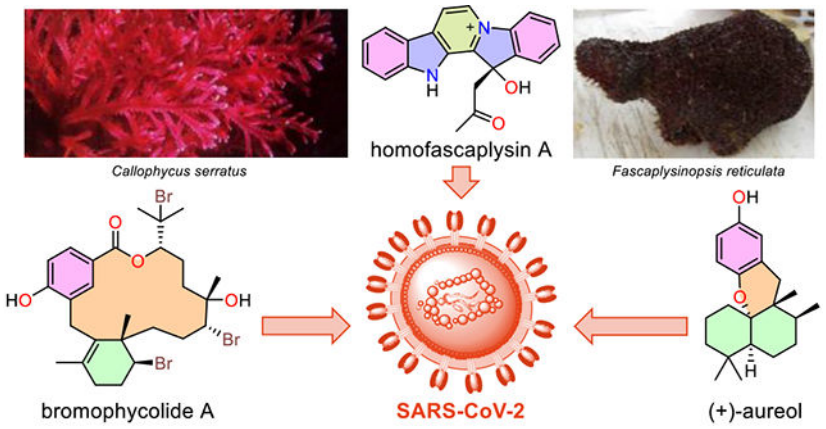

Introduction

COVID-19, caused by infection with the SARS-CoV-2 coronavirus, is a novel disease affecting human populations worldwide that has led to over 5.9 million deaths and 440 million infections as of March, 2022.[1] As the pandemic continues, the deployment of several safe and effective vaccines has brought some optimism. Nevertheless, the only FDA approved direct-acting small molecule antiviral drugs for SARS-CoV-2 are remdesivir, molnupiravir, and a combination therapy using PF-07321332 with ritonavir (PAXLOVID™).[2,3,4,5] Remdesivir has been shown to shorten the recovery time in hospitalized patients, whereas molnupiravir significantly reduces the risk of hospitalization and death. The combination therapy using PF-07321332 with ritonavir has displayed promise in Phase 2-3 clinical trials, reducing the risk of hospitalization by almost 89% and with no deaths.[4] While these developments are promising, controlling virus transmission and treating patients require development of additional therapeutics, including small molecule drug candidates that can be used in combination regimens, a therapeutic approach that has proved beneficial in the fight against human immunodeficiency virus, hepatitis B, and hepatitis C virus.[6] Furthermore, there is the possibility of additional benefits to human health through the discovery of compounds with activity against other coronaviruses. Although morbidity caused by many coronaviruses is mild (coronaviruses cause 10–30% of “common cold” upper respiratory tract infections),[7, 8] SARS-CoV-2 is the third highly virulent coronavirus to emerge in the last 20 years, and it is unlikely to be the last.

In the search for novel drug candidates to treat or prevent COVID-19, a broad assessment of antiviral activities attributed to known marine and terrestrial natural products is a useful starting point for prioritizing screening of compounds against SARS-CoV-2. A wide array of molecules from terrestrial and marine sources show antiviral activity including inhibition of coronaviruses (Figure S1-S2).[9-15] Some of their putative mechanisms of action include the inhibition of the viral spike protein (S) and angiotensin converting enzyme 2 (ACE2) by anthraquinones and tannins (Figure S1, A),[16, 17] inhibition of viral helicase by flavonoids (Figure S1, B),[18] and inhibitory activity against the SARS-CoV chymotrypsin-like protease ($3CL^{pro}$)/ main protease (M^{pro}) and papain-like cysteine protease (PL^{pro}) by alkaloids, flavonoids, and coumarins (Figure S1, C/D).[19-23] Most relevant, recent reports have

demonstrated potent *in vitro* anti-SARS-CoV-2 activity for natural product representatives of isoprenoid, peptide, polyketide, binaphthoquinone, and polyphenol structural classes (Figure 1, B).[24-28] Recently, the repurposed drug plitidepsin (**4**, also known as dehydrodidemnin B, a depsipeptide from the marine ascidian *Aplidium albicans*; Figure 1, B) was shown to be more than 20 times as potent as remdesivir against SARS-CoV-2.[28] Taken together, the molecular diversity represented by natural products holds promise for discovery of novel drug leads to fill the critical need for SARS-CoV-2 and other RNA viruses of pandemic concern.

Result and discussion

We initiated a study of marine natural products from our collection of several thousand marine extract fractions and pure compounds assembled through the National Institutes of Health (NIH) funded International Cooperative Biodiversity Groups (ICBG) program in Fiji and the Solomon Islands starting in 2004. Natural products with structural similarity to known antiviral molecules, especially those with established activity against coronaviruses and other RNA viruses, were prioritized. Homofascaplysin A (**1**) was chosen due to previously reported activity of other β-carboline alkaloids against RNA viruses including HIV and dengue virus.[29-31] Additionally, members of the fascaplysin class (which includes **1**) structurally resemble tryptanthrin (Figure S1, D), an indole quinazoline alkaloid active against human coronavirus NL63.[19] Aureol (**2**) was selected due to its reported anti-influenza activity and because it embodies the sesquiterpene hydroquinone structural class.[32] Moreover, a close structural analog stachyflin (**16**) has shown nanomolar activity against influenza A virus subtype H1N1, further motivating us to prioritize sesquiterpene hydroquinones (Figure S2).[33, 34] Bromophycolide A (**3),** an unusual meroditerpene macrolide, was selected based on its known anti-HIV activity (Figure 1, A).[35] Two other biosynthetically related polycyclic analogs, bromophycoic acid B (**9**) and callophycoic acid B (**10**), were chosen as additional representatives of this natural product family.[36, 37] Likewise, the complex alkaloid haliclonacyclamine A (**11**) was considered based on its reported anti-HIV activity.[38] Finally, peyssonnoside A (**12**) and formoside (**13**) representative of terpene glycosides, and cladophorol A (**14**), and cladophorol G (**15**) representing polyphenols were also chosen, as compounds from these classes have shown activity against human coronavirus 229E, respiratory syncytial virus, influenza A virus, SARS-CoV PL^{pro}, and $3CL^{pro}$ enzyme (Figure S1-S2).[20, 39, 40] Thus, ten unique molecules belonging to five distinct structural classes were selected and purified from our extract library for screening in a SARS-CoV-2 specific assay with live virus in a BSL-3 facility.

Among the ten natural products that were evaluated, three stood out for their promise based on a series of experiments with SARS-CoV-2-infected human lung cancer Calu-3 cells: homofascaplysin A (**1**), aureol (**2**), and bromophycolide A (**3**). These three natural products significantly suppressed viral infection while not killing human lung cells, relative to DMSO as control, at 0.5–1 μM (Figure 3). Follow-up experiments (with the same assay conditions) to further confirm the bioactivity of **1**–**3** also indicated significant suppression of viral infection at concentrations of 2.8 μM for **1** and 10 μM for **2**–**3** (Figure 4). Although formoside (**13**) showed initial promise in reducing infection by SARS-CoV-2 in Calu-3

cells (Figure 3), these data were not replicated in a subsequent experiment (data not shown). Homofascaplysin A (**1**) exhibited promising inhibition of SARS-CoV-2 infection (EC_{50} 1.1 ± 0.4 μM) but suffered from relatively high cytotoxicity (CC_{50} ~5 μM) towards Calu-3 cells (Table 1). Following widely reported variability and cell-type dependencies for antiviral activities, the Calu-3 experiments were complemented with use of human primary airway cells in polarized pseudostratified air-liquid interface cultures. This model accurately recapitulates the biology of airway epithelia *in vivo*.[41, 42] At 2.8 μM, **1** effectively reduced viral load as indicated by the >90% reduction in harvested SARS-CoV-2 RNA compared with dimethyl sulfoxide (DMSO) control (Figure 5, A). Additionally, **1** did not affect adenoviral transduction which was used as a toxicity control (Figure 5, B). However, compounds **2**–**3** were ineffective in this system at a test concentration of 10 μM.

While anti-SARS-CoV-2 inhibitory activities of **1**–**3** are less promising than known anti-SARS-CoV-2 natural products **4**–**8** (Figure 1, B), they are comparable to other anti-SARS-CoV-2 compounds that have recently been reported in the literature, albeit using different host cell systems.[44-48] Homofascaplysin A (**1**), (+)-aureol (**2**), and bromophycolide A (**3**) represent three diverse structural classes of small molecules (β-carboline alkaloids, sesquiterpene hydroquinones, and meroditerpene macrolides, respectively) that offer numerous naturally occurring analogs and opportunities to create synthetic derivatives to pursue optimal antiviral and cytotoxicity profiles for development of lead candidates for treatment or prevention of SARS-CoV-2.[35, 49-56] As all of the studies were done with compound treatment of cells prior to infection, future work could address post-infection antiviral activity. Additionally, upcoming studies could utilize emerging tools such as replicons and virus-like particles to determine the antiviral mechanisms of lead candidates.[57-61]

The β-carboline alkaloid homofascaplysin A (**1**) belongs to the fascaplysin class of natural products which display a range of biological activities.[29, 55] While fascaplysin has historically been known as a potent and selective CDK4 inhibitor, **1** and its congeners show potent antimicrobial, anticancer, and anti-Alzheimer's activity.[55, 62-68] Fascaplysin has also been shown to be a "balanced" opioid receptor agonist with a signaling profile that resembles endorphins, in contrast to "biased" μ opioid receptor agonists like morphine that participate in G protein signaling but weakly engage β-arrestin and endocytic machinery.[69] Additionally, β-carboline alkaloids including harman (**18**), *N*-butylharmine (**19**), harmol (**20**), and 9-*N*-methylharmine (**21**) have reported activity against HIV and dengue virus (Figure S2).[30, 31] Hence, the β-carboline alkaloids are an important family of molecules that have shown promise against a variety of disease targets.

Sesquiterpene hydroquinones as represented by (+)-aureol (**2**) are common among marine organisms. Several analogs of **2** have been isolated through our ICBG project from marine sponges and algae,[70] with numerous natural and synthetic analogs described in the literature.[33, 34, 71-74] Aureol (**2**) has been shown to exhibit anti-influenza activity in earlier studies.[32] Analogs of **2** including stachyflin (**16**),[33, 34] strongylin A (**22**),[73] and peyssonol A (**23**)[75, 76] possess antiviral activity and hence underscore the importance of exploring the sesquiterpene hydroquinone class of compounds for lead optimization against COVID-19. *In vivo* studies on structural analogs of **16** in mice and ferrets (for anti-influenza virus activity)

indicate that the sesquiterpene hydroquinone class is indeed amenable to development as antiviral drug candidates.[77]

Macrocyclic terpenes as represented by bromophycolide A (**3**) are rare in nature, but Fijian red algae of the genus *Callophycus* are a renowned source of structurally complex diterpene-shikimate macrolides with variable halogenation, cyclization, and stereogenic motifs. Moreover, **3** is present at high concentrations in the producing alga, where it plays a role in defense against algal pathogens.[35, 78] Although there have been a few total synthesis efforts geared towards the meroditerpene macrolide core of bromophycolides, a concise total synthetic approach still remains at bay.[79, 80] Additionally, the biosynthetic pathways for **3** and naturally occurring analogs have not yet been deciphered. The bromophycolides display a range of biological activities including antiviral (against HIV-1), antimicrobial (against methicillin-resistant *Staphylococcus aureus,* vancomycin-resistant *Enterococcus faecium*), antimalarial, and anticancer activities. While anti-HIV-1 activity of **3** is marginal (IC_{50} of 9.8 and 9.1 μM against HIV-1 strains 96USHIPS7 and UG/92/029, respectively), **3** shows sub-micromolar blood stage antimalarial activity, targeting heme crystallization in the human malarial parasite *Plasmodium falciparum.*[35, 52] *In vivo* studies showed low toxicity and reasonable bioavailability in a malaria mouse model. However, the molecule suffers from rapid liver metabolism and hence a short *in vivo* half-life.[53] Thus, future studies directed towards optimized analogs of **3** against SARS-CoV-2 can benefit from the pharmacokinetic and pharmacodynamic results reported for **3** in mouse models.

Taken together, the bioactivities observed for **1**–**3** encourage the exploration of compounds within their structural classes and can be envisioned to offer analogs exhibiting potent activity against SARS-CoV-2 via exploitable inhibitory mechanisms, while minimizing cytotoxicity. Whereas all current and future endeavors for antiviral drug discovery require a multifaceted approach, it's worth noting as stated by Dr. Francis S. Collins in a recent *Science* editorial that: "Another lesson is that the necessary short-term dependence on repurposing existing drugs will not often produce true successful outcomes. For the future, we should begin to work on potent oral antivirals against all major classes of potential pathogens, with the goal of having drugs ready for phase 2/3 efficacy trials when the next threat emerges."[81]

Experimental Procedures

General Experimental Procedures

NMR spectral data were acquired on 18.8 T (800 MHz for ^{1}H and 201 MHz for ^{13}C) Bruker Advance IIIHD instrument equipped with a 3 mm triple resonance cryoprobe. Spectra were recorded in DMSO-d_6, $CDCl_3$, and CD_3OD and referenced to the solvent residual peaks (δ_H and δ_C). NMR data were analyzed using MestReNova 11.0.4.

High resolution MS data were acquired on a Thermo Scientific IDX Tribrid mass spectrometer. Low resolution mass spectrometric data was acquired on a Waters Acquity QDa detector equipped with a Waters 2695 separation module. X ray crystallographic data was acquired on an XtaLAB Synergy, Dualflex, HyPix diffractometer. Optical rotation data was acquired in a Jasco-DIP-360 digital polarimeter.

Specimen Collection and Species Identification

Fascaplysinopsis reticulata (G-0633) was collected in 2008 from Thithia locale, Central Lau Island, Fiji (S 17°47′17.9″, W 179°23′52.8″) at a depth of 17 m. It had a conulose structure, medium hard texture with thin brown mucus and was dark brown in color. A Collection photo for *Fascaplysinopsis reticulata* (G-0633) is provided in the supporting information (Figure S3). *Haliclona* sp. (G-1364) was collected in 2016 near Florida Island, Nggela Sule Island, Solomon Islands (S 9°03′05.8″, E 160°04′30.0″). The organism was found growing prolifically on a reef slope at a depth of 42 m. It had a soft texture, black color with rope like morphological appearance and gave off a black exudate. The sponge was unispicular anisotropic with ~ 80 μm oxeas. For each collection, morphological vouchers were preserved in formalin and DNA vouchers were preserved in molecular grade ethanol, and are stored at the University of the South Pacific's Institute of Applied Sciences. Genus and species were assigned by comparison with published morphological traits and by chemotaxonomic comparison based on the natural products literature.[82-84]

Isolation and characterization of natural products

Bromophycolide A (**1**),[35] bromophycoic acid B (**9**),[36] callophycoic acid B (**10**),[37] peyssonnoside A (**12**),[85] formoside (**13**),[86] cladophorol A (**14**), and cladophorol G (**15**)[87] were isolated as part of previously published investigations of marine algae or sponges, and characterized as detailed in earlier reports. All natural products were stored at −20°C until used for the present study. The purity and identity of each compound were confirmed by comparison of ^{1}H NMR spectroscopic data to original reports. Based on ^{1}H NMR spectroscopic data (Figure S4-S6) bioactive compounds **1**–**3** were at least 90% pure. Compound quantities were determined using quantitative ^{1}H NMR (qNMR) wherein the unknown quantity of a natural product was related to a known amount of caffeine (compound and caffeine were dissolved in equal volume of NMR solvent) using a capillary filled with benzene-d_6 as an internal standard.[88]

Isolation of Homofascaplysin A (**1**) and aureol (**2**): *Fascaplysinopsis reticulata* (1180 g) was exhaustively extracted with 50% aqueous methanol followed by methanol. The combined extracts were partially evaporated *in-vacuo* and partitioned with dichloromethane. The dichloromethane extract was further re-partitioned with water. The dichloromethane-soluble extract (3.2 g) was adsorbed on 200-350 mesh silica gel (1:10 loading capacity), in a flash benchtop open column, and eluted with a step gradient of hexanes/ethyl acetate (1:1) to ethyl acetate/methanol (1:1) furnishing six fractions. Fraction 1 (0.5 g) (pooled from 50% hexanes/ethyl acetate to ethyl acetate elutions) was flash chromatographed over 25 g of 200-350 mesh silica gel (gradient: hexanes to ethyl acetate). Further separation of the fraction containing **2** (as monitored with thin layer chromatography) by C18 silica flash benchtop open column chromatography (eluting with a gradient of 95% aqueous methanol to methanol) gave pure **2** as a yellow oil. The remaining combined 50% aqueous methanol and methanol extract (after partitioning with dichloromethane) was adsorbed into HP20SS resin, dried, and desalted with distilled water. Subsequent elution with methanol provided 1.1 g of extract which was adsorbed onto 20.4 g HP20SS resin and eluted with a gradient of 20% aqueous methanol to 100% methanol followed with methanol/acetone (4:1) to 100% acetone to obtain eight fractions. Fraction eluting with 1:1 methanol/water furnished

partially pure **1** (181.6 mg) as a red powder. A portion of this fraction (14.9 mg) was dissolved in chloroform and passed over celite to furnish 2.4 mg of pure **1** as a brown solid. Characterization data for **1**–**2** are reported in supporting information.

Haliclonacyclamine A (**11**): *Haliclona* sp. (750 g wet weight) was exhaustively extracted with methanol and then with dichloromethane. The crude extract (10.4 g) was suspended in 9:1 mixture of methanol/water and partitioned with hexanes to furnish 1.9 g of hexanes-soluble fraction. The methanol/water extract was adjusted to 3:2 methanol/water and partitioned with dichloromethane to provide 2.6 g of dichloromethane-soluble extract. The methanol was evaporated, and the remaining water extract was partitioned with saturated butanol to give 1.5 g of butanol-soluble fraction. The dichloromethane-soluble fraction was subjected to silica gel column chromatography, eluting with hexanes and dichloromethane (0% to 100% dichloromethane step gradient), dichloromethane and ethyl acetate (0% to 100% ethyl acetate step gradient), ethyl acetate and methanol (0% to 100% methanol step gradient), and finally with methanol/water (1:1) with 0.1% trifluoroacetic acid (TFA) in the aqueous portion. The fraction eluting with 1:1 methanol/water, gave **11** (1.1 g) as a white powder. Although the ^{1}H and ^{13}C NMR spectroscopic data for **11** did not entirely align with that reported in literature for haliclonacyclamine A,[89] the structure was confirmed as haliclonacyclamine A based on X-ray crystallographic data (Figure S11).[90] The discrepancy in NMR data is likely due to protonation of the two nitrogen atoms present in **11** in our case. Characterization data for **11** are reported in supporting information.

Viruses and cells

Vero E6 cells (#CRL-1586, ATCC, Manassas, VA, USA) are derived from the epithelium of an African green monkey kidney; they lack type I interferon production and are commonly used to grow virus stocks. Vero E6 cells were cultured in Dulbecco's modified Eagle's medium (DMEM, #10313-021, Gibco, Waltham, MA, USA) supplemented with 10% fetal bovine serum (FBS, #sh30396.03, lot# ag29759488, Cytiva, Marlborough, MA, USA), 2 mM L-glutamine (#25030-081, Gibco, Waltham, MA, USA), 100 units/ml penicillin and 100 μg/ml streptomycin (#400-109, Gemini Bioproducts, West Sacramento, CA, USA) at 37 °C in a humidified incubator supplemented with 5% CO_2. These cells have been used extensively in the lab, over 100 passages.

Calu-3 lung epithelial adenocarcinoma-derived cells (#HTB-55, ATCC, Manassas, VA, USA) were cultured in Eagle's minimal essential medium (#30-2003, ATCC, Manassas, VA, USA) supplemented with 10% FBS, 100 units/ml penicillin and 100 μg/ml streptomycin at 37 °C in a humidified incubator supplemented with 5% CO_2. These cells were purchased for this study and were used at fewer than 20 passages.

Cryopreserved human bronchial epithelial cells (hBECs) from healthy donors (#FC0035, Lifeline Cell Technology, Frederick, MD, USA) cells were propagated in Ex Plus expansion medium (Stemcell Technologies, Cambridge, MA, USA) beginning at passage 3 on flasks coated with PureCol (Sigma-Aldrich, St. Louis, MO, USA) at 37 °C and 5% CO_2 until ~70-80% confluency. Monolayers were generated on collagen-coated (#234154, Sigma-Aldrich, St. Louis, MO, USA) 6.5 mm transwells (#3470, Corning Life Sciences, Durham, NC, USA) by seeding at density of 150,000 cells per insert and maintained under submerged

conditions in Ex Plus medium for 3 days. Apical and basolateral culture solutions were aspirated, and lower chamber fluid replaced with ALI medium (Stemcell Technologies, Cambridge, MA, USA). Air liquid interface conditions were maintained for 21-28 days until monolayers were fully differentiated.

SARS-CoV-2 isolate USA-WA1/2020 (BEI Resources, Manassas, VA, USA) was used in these studies. This represents an early isolate from the COVID-19 pandemic. To produce stocks, a confluent T75 flask of Vero E6 was infected with SARS-CoV-2 then monitored for cytopathic effect (cpe). When marked cpe was observed (typically 2-3 days post infection), viral supernatant was collected, passed through a 0.22 μm filter to remove cell debris, aliquoted and stored at −80 °C. To determine the infectious titer of stocks, Vero E6 cells were seeded in 96-well plates at 20,000 cells per well, then, after 12-24 h they were infected with serially diluted SARS-CoV-2. After 4-8 h, cells were fixed in 4% paraformaldehyde in PBS, then stained with rabbit monoclonal anti-N (#40143-R001, Sino Biologicals, VWR, Radnor, PA, USA) to identify infected cells, and counter-stained with Hoechst-33342 to identify nuclei. Total cell number and infected cell number were determined by imaging with a Cytation 5 automated microscope (Biotek, Winooski, VT, USA) and image analysis using Gen5 Prime software (Biotek, Winooski, VT, USA). The estimated titer was expressed as infectious units per ml.

SARS-CoV-2 antiviral assays

Initial screening and dose response assays: Experiments were performed in 96-well plates. Calu3 cells were seeded at 30,000 cells per well. Cells were treated with compounds 24 h after seeding, at a confluency of 80-90%. They were infected at a low multiplicity of infection (MOI ~0.01) then incubated for 48 h before being fixed and stained for N protein. Total cell count was determined by counter-staining nuclei with Hoechst-33342. Nuclei and infected (N-protein positive) cells were counted using an automated microscope, as described above.

Antiviral activity in primary airways cells: Air-liquid interface cultures of hBECs were infected by the addition of 300 infectious units (determined on Vero E6) of SARS-CoV-2 in 10 μl medium directly to the apical surface. RNA was harvested immediately (for a 0 h, input value) or after culturing for 48 h. Levels of the SARS-CoV-2 N protein RNA (a marker of viral replication) and the host transcript coding RNase P (an internal standard) were determined by reverse-transcription quantitative PCR (RT-qPCR). RNA was extracted using the PureLink RNA Mini Kit (Thermo Fisher Scientific, Waltham, MA, USA) and eluted in a final volume of 100 μl nuclease-free water. Primers and probes were obtained as part of the SARS-CoV-2 Research Use Only qPCR Primer & Probe Kit: N1, N2 & RP (IDT, Coralville, IA, USA). Reactions were prepared with GoTaq Probe RT-qPCR system (#A6121, Promega, Madison, WI, USA) in final volume of 10 μl, with 1 μl extracted RNA, and run on a PicoReal 96 Real-Time PCR System (Thermo Fisher Scientific, Waltham, MA, USA). A ΔΔCt method was used to determine effects on SARS-CoV-2 replication. The difference in cycle threshold (Ct) between N and RNase P was determined for each experimental condition, then compared to the difference observed at 0 h, i.e., before any replication can occur. Fold change is determined by assuming that a reduction in Ct of 1

cycle represents a 2-fold increase in the amount of starting RNA. All experiments were performed with duplicate cultures and duplicate technical replicates for the RT-qPCR. Basic statistical analyses were performed using Microsoft Excel. Bioassay results were plotted using OriginPro software (OriginPro 2021, OriginLab Corporation, Northampton, MA, USA). EC_{50}'s were calculated using the Quest Graph™ IC_{50} Calculator.[91]

Supplementary Material

Refer to Web version on PubMed Central for supplementary material.

Acknowledgement

This work was supported by ICBG grant U19-TW007401 from the NIH and The Nahmias-Schinazi Chair fund at Emory University. The government of Solomon Islands and Fiji are thanked for allowing research and sample collection in their territorial waters. We are grateful to S. Lavoie (Université du Québec à Chicoutimi) for stimulating conversations leading us to this project. We thank J. Bacsa from the X-ray Crystallography Center at Emory University for the acquisition and interpretation of X-ray crystallographic data. S. G. Moore affiliated to the Institute of Bioengineering and Biosciences Systems Mass Spectrometry Core (SyMSC) at Georgia Tech shared expertise on the acquisition of high-resolution mass spectrometric data. L. Gelbaum and J. Leisen (Georgia Tech NMR Center) are acknowledged for NMR assistance. We thank K. Feussner (University of South Pacific) for taxonomic examination of collected sponges.

References

1. WHO Coronavirus (COVID-19) Dashboard. https://covid19.who.int/ (accessed 2022-03-07)
2. FDA Press Announcements Page. https://www.fda.gov/news-events/press-announcements/fda-approves-first-treatment-covid-19 (accessed 2021-11-04)
3. FDA Press Announcements Page. https://www.fda.gov/news-events/press-announcements/coronavirus-covid-19-update-fda-authorizes-additional-oral-antiviral-treatment-covid-19-certain (accessed 2021-12-26).
4. Pfizer Press Releases page. https://www.pfizer.com/news/press-release/press-release-detail/pfizer-receives-us-fda-emergency-use-authorization-novel (accessed 2021-12-26)
5. FDA Press Announcements Page. https://www.fda.gov/news-events/press-announcements/coronavirus-covid-19-update-fda-authorizes-first-oral-antiviral-treatment-covid-19 (accessed 2021-12-26).
6. Hofmann WP; Soriano V; Zeuzem S Antiviral combination therapy for treatment of chronic hepatitis B, hepatitis C, and human immunodeficiency virus infection. In Handbook of Experimental Pharmacology; Antiviral Strategies; Kräusslich HG; Bartenschlager R, Eds.; Springer: Berlin, Heidelberg, 2009; Vol. 189, pp 321–346.
7. van Elden LJ; van Loon AM; van Alphen F; Hendriksen KA; Hoepelman AI; van Kraaij MG; Oosterheert JJ; Schipper P; Schuurman R; Nijhuis M Frequent Detection of Human Coronaviruses in Clinical Specimens from Patients with Respiratory Tract Infection by Use of a Novel Real-Time Reverse-Transcriptase Polymerase Chain Reaction. J. Infect. Dis 2004, 189 (4), 652–657. [PubMed: 14767819]
8. Paules CI; Marston HD; Fauci AS Coronavirus Infections-More Than Just the Common Cold. JAMA. 2020, 323 (8), 707–708. [PubMed: 31971553]
9. Sayed AM; Khattab AR; AboulMagd AM; Hassan HM; Rateb ME; Zaid H; Abdelmohsen UR Nature as a treasure trove of potential anti-SARS-CoV drug leads: a structural/mechanistic rationale. RSC Adv. 2020, 10 (34), 19790–19802. [PubMed: 35685913]
10. Che CT Marine Products as a Source of Antiviral Drug Leads. Drug Dev. Res 1991, 23 (3), 201–218.
11. El Sayed KA Natural Products as Antiviral Agents. In Studies in Natural Products Chemistry; Attaur-Rahman, Ed.; Elsevier: 2000; Vol. 24, pp 473–572.

12. Martinez JP; Sasse F; Brönstrup M; Diez J; Meyerhans A Antiviral drug discovery: broad-spectrum drugs from nature. Nat. Prod. Rep 2015, 32 (1), 29–48. [PubMed: 25315648]

13. Gogineni V; Schinazi RF; Hamann MT Role of Marine Natural Products in the Genesis of Antiviral Agents. Chem. Rev 2015, 115 (18), 9655–9706. [PubMed: 26317854]

14. Islam MT; Sarkar C; El-Kersh DM; Jamaddar S; Uddin SJ; Shilpi JA; Mubarak MS Natural products and their derivatives against coronavirus: A review of the non-clinical and pre-clinical data. Phytother. Res 2020, 34 (10), 2471–2492. [PubMed: 32248575]

15. Christy MP; Uekusa Y; Gerwick L; Gerwick WH Natural Products with Potential to Treat RNA Virus Pathogens Including SARS-CoV-2. J. Nat. Prod 2021, 84 (1), 161–182. [PubMed: 33352046]

16. Ho TY; Wu SL; Chen JC; Li CC; Hsiang CY Emodin blocks the SARS coronavirus spike protein and angiotensin-converting enzyme 2 interaction. Antivir. Res 2007, 74 (2), 92–101. [PubMed: 16730806]

17. Yi L; Li Z; Yuan K; Qu X; Chen J; Wang G; Zhang H; Luo H; Zhu L; Jiang P; Chen L; Shen Y; Luo M; Zuo G; Hu J; Duan D; Nie Y; Shi X; Wang W; Han Y; Li T; Liu Y; Ding M; Deng H; Xu X Small Molecules Blocking the Entry of Severe Acute Respiratory Syndrome Coronavirus into Host Cells. J. Virol 2004, 78 (20), 11334–11339. [PubMed: 15452254]

18. Yu MS; Lee J; Lee JM; Kim Y; Chin YW; Jee JG; Keum YS; Jeong YJ Identification of myricetin and scutellarein as novel chemical inhibitors of the SARS coronavirus helicase, nsP13. Bioorg. Med. Chem. Lett 2012, 22 (12), 4049–4054. [PubMed: 22578462]

19. Tsai YC; Lee CL; Yen HR; Chang YS; Lin YP; Huang SH; Lin CW Antiviral Action of Tryptanthrin Isolated from *Strobilanthes cusia* Leaf against Human Coronavirus NL63. Biomolecules 2020, 10 (3), 366. [PubMed: 32120929]

20. Kim DW; Seo KH; Curtis-Long MJ; Oh KY; Oh JW; Cho JK; Lee KH; Park KH Phenolic phytochemical displaying SARS-CoV papain-like protease inhibition from the seeds of *Psoralea corylifolia*. J. Enzyme Inhib. Med. Chem 2014, 29 (1), 59–63. [PubMed: 23323951]

21. Cho JK; Curtis-Long MJ; Lee KH; Kim DW; Ryu HW; Yuk HJ; Park KH Geranylated flavonoids displaying SARS-CoV papain-like protease inhibition from the fruits of *Paulownia tomentosa*. Bioorg. Med. Chem 2013, 21 (11), 3051–3057. [PubMed: 23623680]

22. Park JY; Kim JH; Kim YM; Jeong HJ; Kim DW; Park KH; Kwon HJ; Park SJ; Lee WS; Ryu YB Tanshinones as selective and slow-binding inhibitors for SARS-CoV cysteine proteases. Bioorg. Med. Chem 2012, 20 (19), 5928–5935. [PubMed: 22884354]

23. Park JY; Yuk HJ; Ryu HW; Lim SH; Kim KS; Park KH; Ryu YB; Lee WS Evaluation of polyphenols from *Broussonetia papyrifera* as coronavirus protease inhibitors. J. Enzyme Inhib. Med. Chem 2017, 32 (1), 504–515. [PubMed: 28112000]

24. Sa-Ngiamsuntorn K; Suksatu A; Pewkliang Y; Thongsri P; Kanjanasirirat P; Manopwisedjaroen S; Charoensutthivarakul S; Wongtrakoongate P; Pitiporn S; Chaopreecha J; Kongsomros S; Jearawuttanakul K; Wannalo W; Khemawoot P; Chutipongtanate S; Borwornpinyo S; Thitithanyanont A; Hongeng S Anti-SARS-CoV-2 Activity of *Andrographis paniculata* Extract and Its Major Component Andrographolide in Human Lung Epithelial Cells and Cytotoxicity Evaluation in Major Organ Cell Representatives. J. Nat. Prod 2021, 84 (4), 1261–1270. [PubMed: 33844528]

25. Xie X; Lu S; Pan X; Zou M; Li F; Lin H; Hu J; Fan S; He J Antiviral Bafilomycins from a Feces-Inhabiting *Streptomyces* sp. J. Nat. Prod 2021, 84 (2), 537–543. [PubMed: 33631936]

26. Ashhurst AS; Tang AH; Fajtová P; Yoon MC; Aggarwal A; Bedding MJ; Stoye A; Beretta L; Pwee D; Drelich A; Skinner D; Li L; Meek TD; McKerrow JH; Hook V; Tseng CT; Larance M; Turville S; Gerwick WH; O'Donoghue AJ; Payne RJ Potent Anti-SARS-CoV-2 Activity by the Natural Product Gallinamide A and Analogues via Inhibition of Cathepsin L. J. Med. Chem 2021.

27. Li YT; Yang C; Wu Y; Lv JJ; Feng X; Tian X; Zhou Z; Pan X; Liu S; Tian LW Axial Chiral Binaphthoquinone and Perylenequinones from the Stromata of *Hypocrella bambusae* Are SARS-CoV-2 Entry Inhibitors. J. Nat. Prod 2021, 84 (2), 436–443. [PubMed: 33560122]

28. White KM; Rosales R; Yildiz S; Kehrer T; Miorin L; Moreno E; Jangra S; Uccellini MB; Rathnasinghe R; Coughlan L; Martinez-Romero C; Batra J; Rojc A; Bouhaddou M; Fabius JM; Obernier K; Dejosez M; Guillén MJ; Losada A; Avilés P; Schotsaert M; Zwaka T; Vignuzzi

M; Shokat KM; Krogan NJ; García-Sastre A Plitidepsin has potent preclinical efficacy against SARS-CoV-2 by targeting the host protein eEF1A. Science 2021, 371 (6532), 926–931. [PubMed: 33495306]

29. Kirsch G; Köng GM; Wright AD; Kaminsky R A new bioactive sesterterpene and antiplasmodial alkaloids from the marine sponge *Hyrtios* cf. *erecta*. J. Nat. Prod 2000, 63 (6), 825–829. [PubMed: 10869210]
30. Ishida J; Wang HK; Oyama M; Cosentino ML; Hu CQ; Lee KH Anti-AIDS agents. 46.[1] Anti-HIV Activity of Harman, an Anti-HIV Principle from *Symplocos setchuensis,* and Its Derivatives. J. Nat. Prod 2001, 64 (7), 958–960. [PubMed: 11473435]
31. Quintana VM; Piccini LE; Panozzo Zénere JD; Damonte EB; Ponce MA; Castilla V Antiviral activity of natural and synthetic β-carbolines against dengue virus. Antivir. Res 2016, 134, 26–33. [PubMed: 27568370]
32. Wright AE; Cross SS; Burres N; Koehn F Novel antiviral and antitumor terpene hydroquinones and methods of use. US patent 5,051,519, 1991.
33. Minagawa K; Kouzuki S; Yoshimoto J; Kawamura Y; Tani H; Iwata T; Terui Y; Nakai H; Yagi S; Hattori N; Fujiwara T; Kamigauchi T Stachyflin and Acetylstachyflin, Novel Anti-influenza A Virus Substances, Produced by *Stachybotrys* sp. RF-7260. I. Isolation, Structure Elucidation and Biological Activities. J. Antibiot 2002, 55 (2), 155–164.
34. Minagawa K; Kouzuki S; Kamigauchi T Stachyflin and Acetylstachyflin, Novel Anti-influenza A Virus Substances, Produced by *Stachybotrys* sp. RF-7260. II. Synthesis and Preliminary Structure-Activity Relationships of Stachyflin Derivatives. J. Antibiot 2002, 55 (2), 165–171.
35. Kubanek J; Prusak AC; Snell TW; Giese RA; Hardcastle KI; Fairchild CR; Aalbersberg W; Raventos-Suarez C; Hay ME Antineoplastic Diterpene-Benzoate Macrolides from the Fijian Red Alga *Callophycus serratus*. Org. Lett 2005, 7 (23), 5261–5264. [PubMed: 16268553]
36. Teasdale ME; Shearer TL; Engel S; Alexander TS; Fairchild CR; Prudhomme J; Torres M; Le Roch K; Aalbersberg W; Hay ME; Kubanek J Bromophycoic acids: Bioactive natural products from a Fijian red alga *Callophycus* sp. J. Org. Chem 2012, 77 (18), 8000–8006. [PubMed: 22920243]
37. Lane AL; Stout EP; Hay ME; Prusak AC; Hardcastle K; Fairchild CR; Franzblau SG; Le Roch K; Prudhomme J; Aalbersberg W; Kubanek J Callophycoic Acids and Callophycols from the Fijian Red Alga *Callophycus serratus*. J. Org. Chem 2007, 72 (19), 7343–7351. [PubMed: 17715978]
38. Tietjen I; Williams DE; Read S; Kuang XT; Mwimanzi P; Wilhelm E; Markle T; Kinloch NN; Naphen CN; Tenney K; Mesplède T; Wainberg MA; Crews P; Bell B; Andersen RJ; Brumme ZL; Brockman MA Inhibition of NF-κB-dependent HIV-1 replication by the marine natural product bengamide A. Antivir. Res 2018, 152, 94–103. [PubMed: 29476895]
39. Cheng PW; Ng LT; Chiang LC; Lin CC Antiviral Effects of Saikosaponins on Human Coronavirus 229E *in vitro*. Clin. Exp. Pharmacol. Physiol 2006, 33 (7), 612–616. [PubMed: 16789928]
40. Ubillas R; Jolad SD; Bruening RC; Kernan MR; King SR; Sesin DF; Barrett M; Stoddart CA; Flaster T; Kuo J; Ayala F; Meza E; Castañel M; McMeekin D; Rozhon E; Tempesta MS; Barnard D; Huffman J; Smee D; Sidwell R; Soike K; Brazier A; Safrin S; Orlando R; Kenny PT; Berova N; Nakanishi K SP-303, an Antiviral Oligomeric Proanthocyanidin from the Latex of *Croton lechleri* (Sangre de Drago). Phytomedicine 1994, 1 (2), 77–106. [PubMed: 23195881]
41. Zhu N; Zhang D; Wang W; Li X; Yang B; Song J; Zhao X; Huang B; Shi W; Lu R; Niu P; Zhan F; Ma X; Wang D; Xu W; Wu G; Gao GF; Tan W A novel coronavirus from patients with pneumonia in China, 2019. N. Engl. J. Med 2020, 382 (8), 727–733. [PubMed: 31978945]
42. Leung C; Wadsworth SJ; Yang SJ; Dorscheid DR Structural and functional variations in human bronchial epithelial cells cultured in air-liquid interface using different growth media. Am. J. Physiol. Lung Cell. Mol. Physiol 2020, 318 (5), L1063–L1073. [PubMed: 32208929]
43. Dittmar M; Lee JS; Whig K; Segrist E; Li M; Kamalia B; Castellana L; Ayyanathan K; Cardenas-Diaz FL; Morrisey EE Drug repurposing screens reveal cell-type-specific entry pathways and FDA-approved drugs active against SARS-Cov-2. Cell Rep. 2021, 35 (1), 108959. [PubMed: 33811811]
44. Abdallah HM; El-Halawany AM; Sirwi A; El-Araby AM; Mohamed GA; Ibrahim SRM; Koshak AE; Asfour HZ; Awan ZA; M AE Repurposing of Some Natural Product Isolates as SARS-

COV-2 Main Protease Inhibitors via In Vitro Cell Free and Cell-Based Antiviral Assessments and Molecular Modeling Approaches. Pharmaceuticals 2021, 14 (3), 213. [PubMed: 33806331]

45. Chen Z; Cui Q; Cooper L; Zhang P; Lee H; Chen Z; Wang Y; Liu X; Rong L; Du R Ginkgolic acid and anacardic acid are specific covalent inhibitors of SARS-CoV-2 cysteine proteases. Cell Biosci. 2021, 11, 45. [PubMed: 33640032]
46. Cao R; Hu H; Li Y; Wang X; Xu M; Liu J; Zhang H; Yan Y; Zhao L; Li W; Zhang T; Xiao D; Guo X; Li Y; Yang J; Hu Z; Wang M; Zhong W Anti-SARS-CoV-2 Potential of Artemisinins In Vitro. ACS. Infect. Dis 2020, 6 (9), 2524–2531. [PubMed: 32786284]
47. Raj v.; Park JG; Cho KH; Choi P; Kim T; Ham J; Lee J Assessment of antiviral potencies of cannabinoids against SARS-CoV-2 using computational and *in vitro* approaches. Int. J. Biol. Macromol 2021, 168, 474–485. [PubMed: 33290767]
48. Yang L; Wang Z Natural Products, Alone or in Combination with FDA-Approved Drugs, to Treat COVID-19 and Lung Cancer. Biomedicines 2021, 9 (6), 689. [PubMed: 34207313]
49. Kubanek J; Prusak AC; Snell TW; Giese RA; Fairchild CR; Aalbersberg W; Hay ME Bromophycolides C-I from the Fijian red alga *Callophycus serratus*. J. Nat. Prod 2006, 69 (5), 731–735. [PubMed: 16724831]
50. Lane AL; Stout EP; Lin AS; Prudhomme J; Le Roch K; Fairchild CR; Franzblau SG; Hay ME; Aalbersberg W; Kubanek J Antimalarial Bromophycolides J-Q from the Fijian Red Alga *Callophycus serratus*. J. Org. Chem 2009, 74 (7), 2736–2742. [PubMed: 19271727]
51. Lin AS; Stout EP; Prudhomme J; Le Roch K; Fairchild CR; Franzblau SG; Aalbersberg W; Hay ME; Kubanek J Bioactive Bromophycolides R-U from the Fijian Red Alga *Callophycus serratus*. J. Nat. Prod 2010, 73 (2), 275–278. [PubMed: 20141173]
52. Stout EP; Cervantes S; Prudhomme J; France S; La Clair JJ; Le Roch K; Kubanek J Bromophycolide A Targets Heme Crystallization in the Human Malaria Parasite *Plasmodium falciparum*. ChemMedChem. 2011, 6 (9), 1572–1577. [PubMed: 21732541]
53. Teasdale ME; Prudhomme J; Torres M; Braley M; Cervantes S; Bhatia SC; La Clair JJ; Le Roch K; Kubanek J Pharmacokinetics, Metabolism, and *in vivo* Efficacy of the Antimalarial Natural Product Bromophycolide A. ACS Med. Chem. Lett 2013, 4 (10), 989–993. [PubMed: 24159368]
54. Djura P; Stierle DB; Sullivan B; Faulkner DJ; Arnold EV; Clardy J Some Metabolites of the Marine Sponges *Smenospongia aurea* and *Smenospongia* (. ident. *Polyfibrospongia*) *echina*. J. Org. Chem 1980, 45 (8), 1435–1441.
55. Segraves NL; Robinson SJ; Garcia D; Said SA; Fu X; Schmitz FJ; Pietraszkiewicz H; Valeriote FA; Crews P Comparison of Fascaplysin and Related Alkaloids: A Study of Structures, Cytotoxicities, and Sources. J. Nat. Prod 2004, 67 (5), 783–792. [PubMed: 15165138]
56. Wildermuth R; Speck K; Haut F-L; Mayer P; Karge B; Brönstrup M; Magauer T A modular synthesis of tetracyclic meroterpenoid antibiotics. Nat. Commun 2017, 8 (1), 1–9. [PubMed: 28232747]
57. Ricardo-Lax I; Luna JM; Thao TTN; Le Pen J; Yu Y; Hoffmann H-H; Schneider WM; Razooky BS; Fernandez-Martinez J; Schmidt F Replication and single-cycle delivery of SARS-CoV-2 replicons. Science 2021, 374 (6571), 1099–1106. [PubMed: 34648371]
58. Xia H; Cao Z; Xie X; Zhang X; Chen JY-C; Wang H; Menachery VD; Rajsbaum R; Shi P-Y Evasion of type I interferon by SARS-CoV-2. Cell Rep. 2020, 33 (1), 108234. [PubMed: 32979938]
59. He X; Quan S; Xu M; Rodriguez S; Goh SL; Wei J; Fridman A; Koeplinger KA; Carroll SS; Grobler JA; Espeseth AS; Olsen DB; Hazuda DJ; Wang D Generation of SARS-CoV-2 reporter replicon for high-throughput antiviral screening and testing. Proc. Natl. Acad. Sci. U.S.A 2021, 118 (15), e2025866118. [PubMed: 33766889]
60. Zhao X; Chen D; Szabla R; Zheng M; Li G; Du P; Zheng S; Li X; Song C; Li R; Guo JT; Junop M; Zeng H; Lin H Broad and Differential Animal Angiotensin-Converting Enzyme 2 Receptor Usage by SARS-CoV-2. J. Virol 2020, 94 (18), e00940–20. [PubMed: 32661139]
61. Zhang X; Liu Y; Liu J; Bailey AL; Plante KS; Plante JA; Zou J; Xia H; Bopp NE; Aguilar PV A trans-complementation system for SARS-CoV-2 recapitulates authentic viral replication without virulence. Cell 2021, 184 (8), 2229–2238. [PubMed: 33691138]

62. Pan H; Qiu H; Zhang K; Zhang P; Liang W; Yang M; Mou C; Lin M; He M; Xiao X; Zhang D; Wang H; Liu F; Li Y; Jin H; Yan X; Liang H; Cui W Fascaplysin Derivatives Are Potent Multitarget Agents against Alzheimer's Disease: *in Vitro* and *in Vivo* Evidence. ACS Chem. Neurosci 2019, 10 (11), 4741–4756. [PubMed: 31639294]
63. Manda S; Sharma S; Wani A; Joshi P; Kumar V; Guru SK; Bharate SS; Bhushan S; Vishwakarma RA; Kumar A; Bharate SB Discovery of a marine-derived bis-indole alkaloid fascaplysin, as a new class of potent P-glycoprotein inducer and establishment of its structure-activity relationship. Eur. J. Med. Chem 2016, 107, 1–11. [PubMed: 26560048]
64. Soni R; Muller L; Furet P; Schoepfer J; Stephan C; Zumstein-Mecker S; Fretz H; Chaudhuri B Inhibition of Cyclin-Dependent Kinase 4 (Cdk4) by Fascaplysin, a Marine Natural Product. Biochem. Biophys. Res. Commun 2000, 275 (3), 877–884. [PubMed: 10973815]
65. Sharma S; Guru SK; Manda S; Kumar A; Mintoo MJ; Prasad VD; Sharma PR; Mondhe DM; Bharate SB; Bhushan S A marine sponge alkaloid derivative 4-chloro fascaplysin inhibits tumor growth and VEGF mediated angiogenesis by disrupting PI3K/Akt/mTOR signaling cascade. Chem.-Biol. Interact 2017, 275, 47–60. [PubMed: 28756150]
66. Bharate SB; Manda S; Mupparapu N; Battini N; Vishwakarma RA Chemistry and Biology of Fascaplysin, a Potent Marine-Derived CDK-4 Inhibitor. Mini-Rev. Med. Chem 2012, 12 (7), 650–664. [PubMed: 22512549]
67. Zhidkov ME; Smirnova PA; Tryapkin OA; Kantemirov AV; Khudyakova YV; Malyarenko OS; Ermakova SP; Grigorchuk VP; Kaune M; Amsberg GV; Dyshlovoy SA Total Syntheses and Preliminary Biological Evaluation of Brominated Fascaplysin and Reticulatine Alkaloids and Their Analogues. Mar. Drugs 2019, 17 (9), 496. [PubMed: 31450717]
68. Lu Z; Ding Y; Li XC; Djigbenou DR; Grimberg BT; Ferreira D; Ireland CM; Van Wagoner RM 3-bromohomofascaplysin A, a fascaplysin analogue from a Fijian *Didemnum* sp. ascidian. Bioorg. Med. Chem 2011, 19 (22), 6604–6607. [PubMed: 21696970]
69. Johnson TA; Milan-Lobo L; Che T; Ferwerda M; Lambu E; McIntosh NL; Li F; He L; Lorig-Roach N; Crews P; Whistler JL Identification of the First Marine-Derived Opioid Receptor "Balanced" Agonist with a Signaling Profile That Resembles the Endorphins. ACS Chem. Neurosci 2017, 8 (3), 473–485. [PubMed: 27744679]
70. Lane AL; Mular L; Drenkard EJ; Shearer TL; Engel S; Fredericq S; Fairchild CR; Prudhomme J; Le Roch K; Hay ME; Aalbersberg W; Kubanek J Ecological leads for natural product discovery: Novel sesquiterpene hydroquinones from the red macroalga *Peyssonnelia* sp. Tetrahedron 2010, 66 (2), 455–461. [PubMed: 20661312]
71. Shen YC; Liaw CC; Ho JR; Khalil AT; Kuo YH Isolation of aureol from *Smenospongia* sp. and cytotoxic activity of some aureol derivatives. Nat. Prod. Res 2006, 20 (6), 578–585. [PubMed: 16835091]
72. Hamann MT Enhancing Marine Natural Product Structural Diversity and Bioactivity through Semisynthesis and Biocatalysis. Curr. Pharm. Des 2003, 9 (11), 879–889. [PubMed: 12678872]
73. Wright AE; Rueth SA; Cross SS An Antiviral Sesquiterpene Hydroquinone from the Marine Sponge *Strongylophora hartmani*. J. Nat. Prod 1991, 54 (4), 1108–1111. [PubMed: 1791476]
74. Utkina NK; Denisenko VA; Scholokova OV; Virovaya MV; Prokof'eva NG Cyclosmenospongine, a new sesquiterpenoid aminoquinone from an Australian marine sponge *Spongia* sp. Tetrahedron Lett. 2003, 44 (1), 101–102.
75. Loya S; Bakhanashvili M; Kashman Y; Hizi A Peyssonols A and B, Two Novel Inhibitors of the Reverse Transcriptases of Human Immunodeficiency Virus Types 1 and 2. Arch. Biochem. Biophys 1995, 316 (2), 789–796. [PubMed: 7532386]
76. Treitler DS; Li Z; Krystal M; Meanwell NA; Snyder SA Evaluation of HIV-1 inhibition by stereoisomers and analogues of the sesquiterpenoid hydroquinone peyssonol A. Bioorg. Med. Chem. Lett 2013, 23 (7), 2192–2196. [PubMed: 23434230]
77. Yoshimoto J; Yagi S; Ono J; Sugita K; Hattori N; Fujioka T; Fujiwara T; Sugimoto H; Hashimoto N Development of Anti-influenza Drugs: II. Improvement of Oral and Intranasal Absorption and the Anti-influenza Activity of Stachyflin Derivatives. J. Pharm. Pharmacol 2000, 52 (10), 1247–1255. [PubMed: 11092569]

78. Lane AL; Nyadong L; Galhena AS; Shearer TL; Stout EP; Parry RM; Kwasnik M; Wang MD; Hay ME; Fernandez FM; Kubanek J Desorption electrospray ionization mass spectrometry reveals surface-mediated antifungal chemical defense of a tropical seaweed. Proc. Natl. Acad. Sci. U.S.A 2009, 106 (18), 7314–7319. [PubMed: 19366672]

79. Lin H; Pochapsky SS; Krauss IJ A Short Asymmetric Route to the Bromophycolide A and D Skeleton. Org. Lett 2011, 13 (5), 1222–1225. [PubMed: 21309525]

80. Bahou KA; Braddock DC; Meyer AG; Savage GP Relay Cross Metathesis for the Iterative Construction of Terpenoids and Synthesis of a Diterpene-Benzoate Macrolide of Biogenetic Relevance to the Bromophycolides. Org. Lett 2020, 22 (8), 3176–3179. [PubMed: 32227974]

81. Collins FS COVID-19 lessons for research. Science 2021, 371 (6534), 1081. [PubMed: 33707241]

82. de Voogd NJAB; Boury-Esnault N; Carballo JL; Cárdenas P; Díaz M-C; Dohrmann M; Downey R; Hajdu E; Hooper JNA; Kelly M; Klautau M; Manconi R; Morrow CC Pisera AB; Rios P; Rützler K; Schönberg C; Vacelet J; van Soest RWM (2022). World Porifera Database. *Fascaplysinopsis reticulata* (Hentschel, 1912). Accessed through: World Register of Marine Species at: https://www.marinespecies.org/aphia.php?p=taxdetails&id=165315 on 2022-03-06.

83. Qin G-F; Tang X-L; de Voogd NJ; Li P-L; Li G-Q Cytotoxic components from the Xisha sponge *Fascaplysinopsis reticulata*. Nat. Prod. Res 2020, 34 (6), 790–796. [PubMed: 30445862]

84. Charan RD; Garson MJ; Brereton IM; Willis AC; Hooper JN Haliclonacyclamines A and B, cytotoxic alkaloids from the tropical marine sponge *Haliclona* sp. Tetrahedron 1996, 52 (27), 9111–9120.

85. Khatri Chhetri B; Lavoie S; Sweeney-Jones AM; Mojib N; Raghavan V; Gagaring K; Dale B; McNamara CW; Soapi K; Quave CL; Polavarapu PL; Kubanek J Peyssonnosides A-B, Unusual Diterpene Glycosides with a Sterically Encumbered Cyclopropane Motif: Structure Elucidation Using an Integrated Spectroscopic and Computational Workflow. J. Org. Chem 2019, 84 (13), 8531–8541. [PubMed: 31244158]

86. Kubanek J; Pawlik JR; Eve TM; Fenical W Triterpene glycosides defend the Caribbean reef sponge *Erylus formosus* from predatory fishes. Mar. Ecol. Prog. Ser 2000, 207, 69–77.

87. Lavoie S; Sweeney-Jones AM; Mojib N; Dale B; Gagaring K; McNamara CW; Quave CL; Soapi K; Kubanek J Antibacterial Oligomeric Polyphenols from the Green Alga *Cladophora socialis*. J. Org. Chem 2019, 84 (9), 5035–5045. [PubMed: 30908914]

88. Bharti SK; Roy R Quantitative ^{1}H NMR spectroscopy. Trends Anal. Chem 2012, 35, 5–26.

89. Clark RJ; Field KL; Charan RD; Garson MJ; Brereton M; Willis AC The Haliclonacyclamines, Cytotoxic Tertiary Alkaloids from the Tropical Marine Sponge *Haliclona* sp. Tetrahedron 1998, 54 (30), 8811–8826.

90. Mudianta IW; Garson MJ; Bernhardt PV The Absolute Configurations of Haliclonacyclamines A and B Determined by X-ray Crystallographic Analysis. Aust. J. Chem 2009, 62 (7), 667–670.

91. "Quest Graph™ IC50 Calculator." AAT Bioquest, Inc., 11 Aug. 2021, https://www.aatbio.com/tools/ic50-calculator.

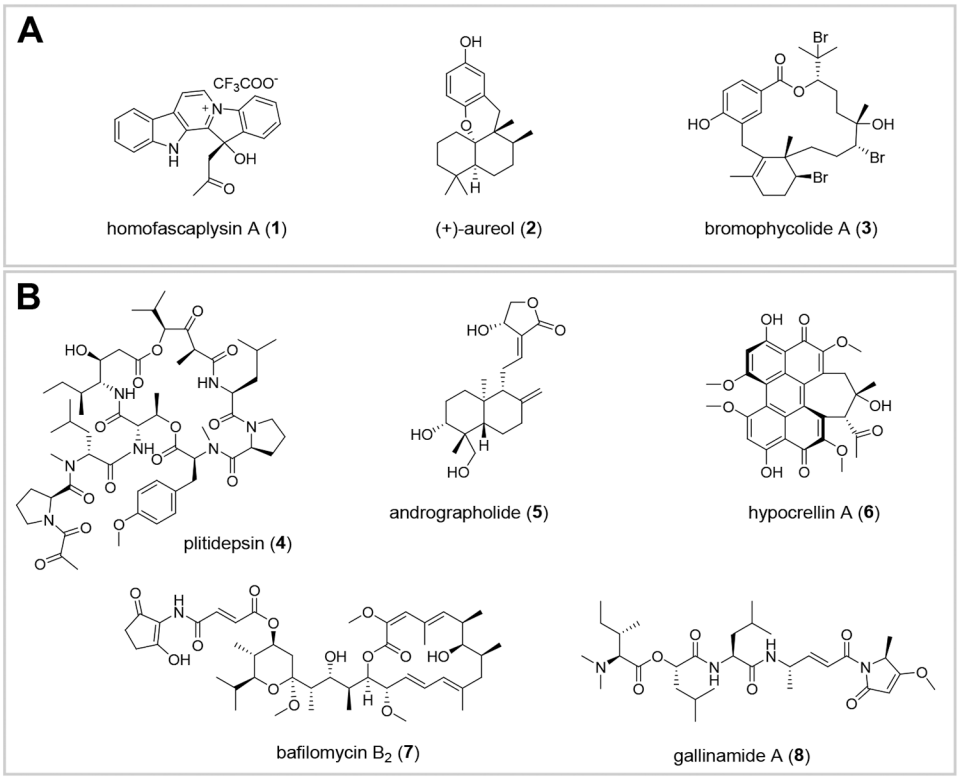

Figure 1.

A: Homofascaplysin A (**1**), (+)-aureol (**2**), and bromophycolide A ***(3),*** which exhibited anti SARS-CoV-2 activity in the current study. **B**: Natural products recently reported to show potent activity against SARS-CoV-2.[24-28]

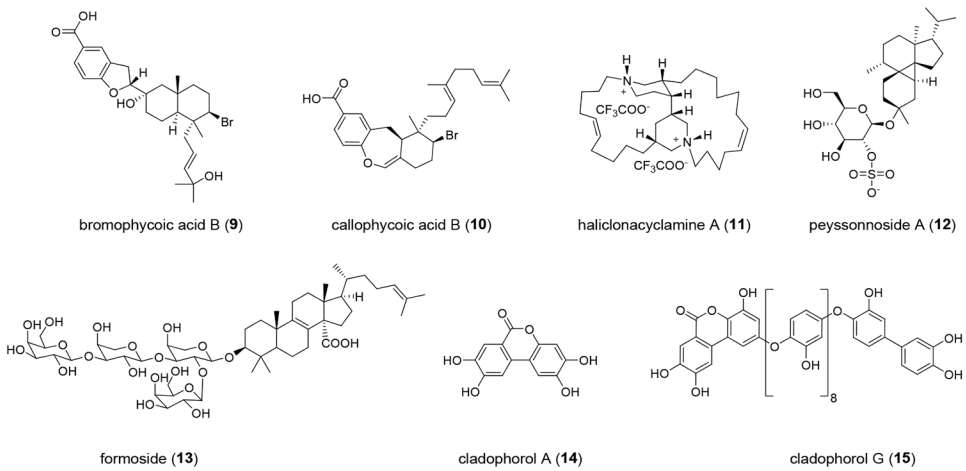

Figure 2.

Natural products screened with a SARS-CoV-2 live virus assay in the present study, in addition to those in Figure 1, A).

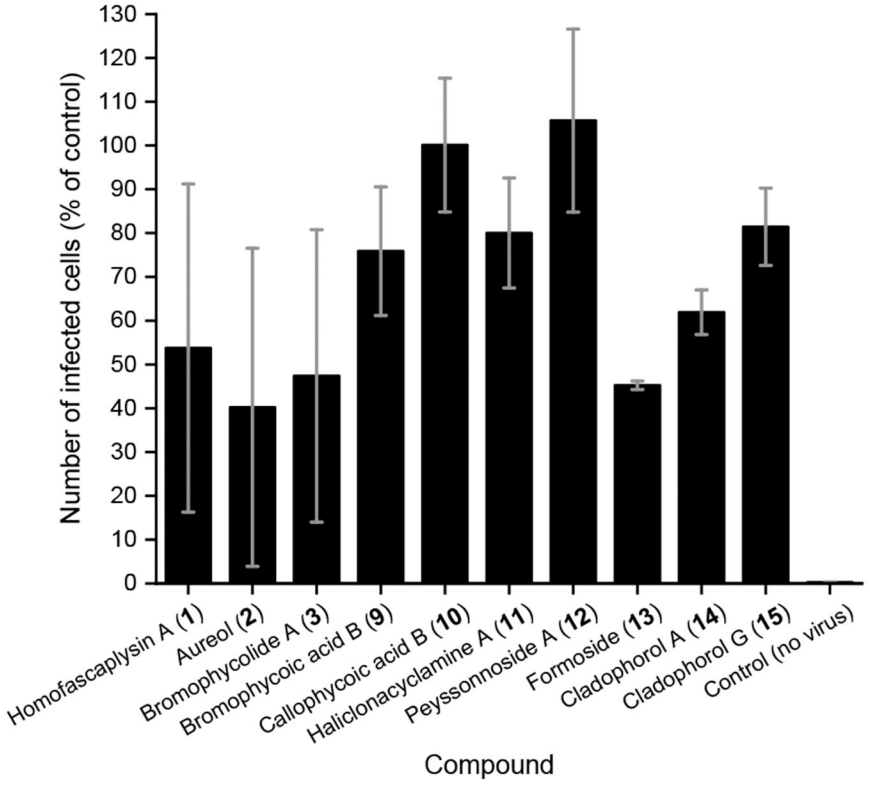

Figure 3.

Inhibition of SARS-CoV-2 infection by ten natural products in human lung cancer Calu-3 cells. All compounds were prepared in 100% DMSO and used at a final concentration of 1 μM (1% DMSO) except for homofascaplysin A (**1**, 0.5 μM), cladophorol A (**14**, 10 μM), and cladophorol G (**15**, 10 μM). Following treatment with the compounds, cells were infected with SARS-CoV-2. After 48 h, cells were fixed and stained to visualize SARS-CoV-2 infected cells and nuclei. Both infected and uninfected cells were counted by automated microscopy; within each experiment, the number of total cells present at the end of the experiment was similar across all treatments (data not shown). 1% DMSO was used as vehicle control. Mean of two independent experiments are shown with standard error of the mean.

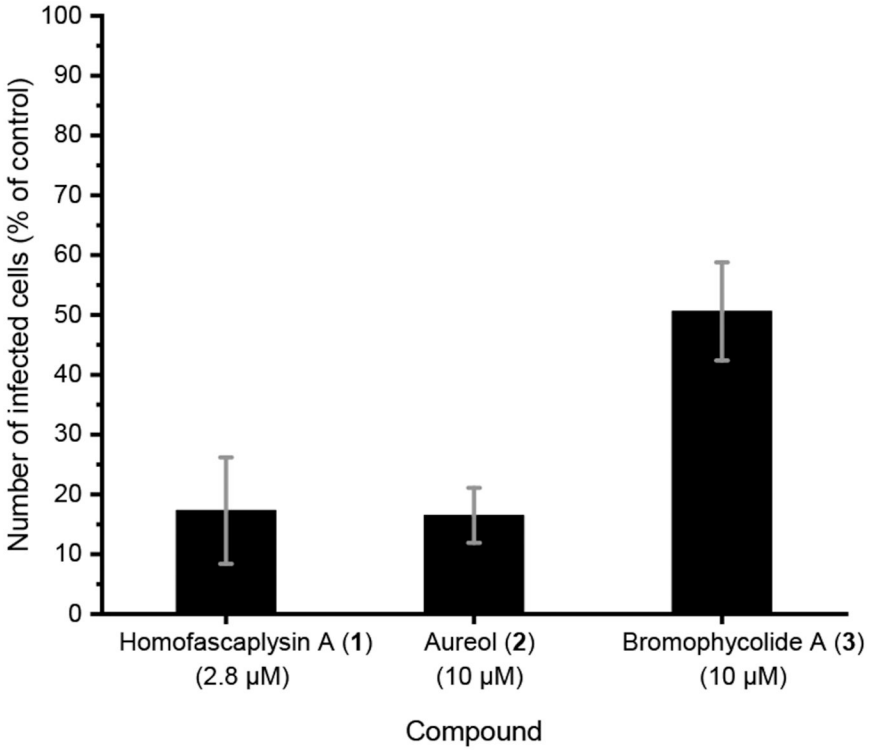

Figure 4.

Inhibition of SARS-CoV-2 infection in human lung cancer Calu-3 cells, performed as for Figure 3. Calu-3 cells were treated with the indicated compounds in a final concentration of 1% DMSO. Mean of two independent experiments shown with standard error of the mean.

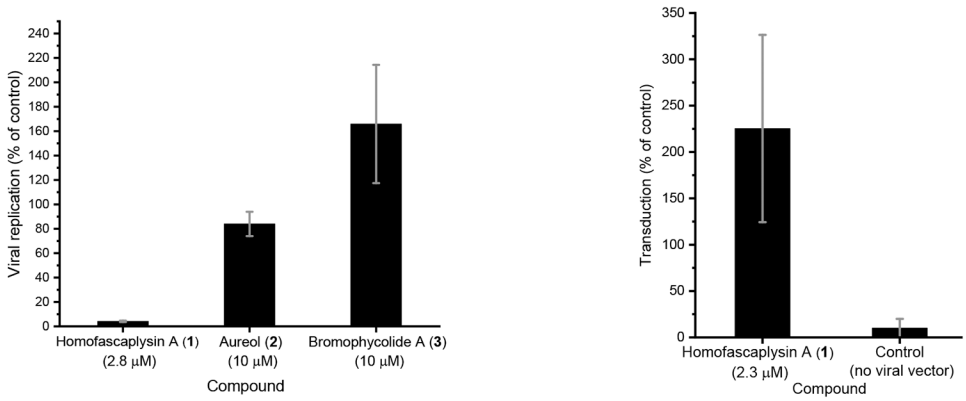

Figure 5.

Inhibition of SARS-CoV-2 infection by natural products in primary human airway cells. **A**) Primary human airway cells in air-liquid interface culture were treated with **1** in a final concentration of 0.1% DMSO and with **2**–**3** in a final concentration of 1 % DMSO. Compounds were added to the basal medium 1 h prior to infection. 1000 infectious units of SARS-CoV-2 was added to the apical surface of the cells. Total RNA was harvested at 0 h (input) and 48 h post-infection, replication was defined as the increase in viral RNA from 0 to 48 h relative to the corresponding DMSO sample. Averaged data from 2 independent experiments shown with standard error of the mean. **B**) Primary human airway cells in air-liquid interface culture were treated with **1** in a final concentration of 0.1% DMSO and added to the basal medium 1 h prior to transduction with 10,000 infectious units of an adenoviral vector containing a CMV-driven GFP. After 48 h, cells were imaged and number of GFP expressing cells was counted; number of transduced cells was expressed relative to the DMSO treated sample. Averaged data from two independent experiments shown with standard error of the mean. Similar results were observed at 2.8 μM of **1** (single independent experiment).

Table 1.

SARS-CoV-2 inhibition in human Calu-3 cells by **1**–**3**.

Compound	EC_{50} (μM) [a]	CC_{50} (μM) [a]
Homofascaplysin A (**1**)	1.1 ± 0.4	~5
(+)-Aureol (**2**)	4.0 ± 1.0	>10
Bromophycolide A (**3**)	6.9 ± 2.0	>10
Remdesivir	0.3	>5 [b]
DMSO control	8.3 ± 1.5	>10

[a] EC_{50} and CC_{50} were determined from dose response in Calu-3 cells. Averages from three independent experiments shown with standard error of the mean.

[b] Literature precedent shows that CC_{50} for remdesivir was >40 μM against Calu-3 cells.[43]